COHERENCE ESTIMATES FROM SYNTHETIC APERTURE SONAR

JL Prater Naval Surface Warfare Center Panama City Division, Panama City, FL, USA

1 INTRODUCTION

Imaging sonar technology has significantly matured to the point where short-range high resolution real aperture sonar (RAS) systems are relatively common. These systems produce imagery by beamforming data, a process generally comprised of a coherent summation of the array data for a given range bin to increase the directivity of the response[1]. The data for all channels of the array are collected simultaneously for a given range bin. Therefore phase shifts along the array are well understood and determined by the geometry of the system. This results in well focused imagery where incoherence (*i.e.* array data that is out of phase compared to an expected value) during beamforming is rarely observed.

Production of sonar imagery at long range requires lower frequencies in order to reduce attenuation. Long-range systems also require proportionally longer apertures to achieve similar resolution relative to short-range higher-frequency RAS systems. Synthetic aperture sonar (SAS) systems have been developed to provide long apertures where RAS designs are impractical. With SAS systems, the data used for image formation is acquired over multiple pings prior to beamforming[2]. As SAS technology has matured, these systems have demonstrated high resolution long range performance across many environments[3].

Since SAS data is acquired over short, non-instantaneous, time spans, SAS data is subject to incoherence that may be caused by unwanted system motion, motion of the imaged objects, or environmental phenomena that cause deviations in the propagated sound path compared with an idealized path assumed in beamforming algorithms. Incoherent samples along the synthetic array will result in reduced image quality[3]. Considering that image quality can vary with environmental or system configurations, metrics have been developed that respond to changes in SAS image quality[4,5], and in some cases the metrics have been related to array coherence[4].

In order to provide consistent high-quality imagery, developers have conducted research focused on the mitigation of unwanted incoherence[6]. These efforts have primarily focused on the development of motion estimation and compensation and autofocus algorithms. In these techniques, phase shifts are observed in the data and algorithms are applied to realign the data to enable fully coherent synthetic apertures in order to provide optimal system performance. While the algorithms described above are beyond the scope of this paper, we suggest that the intermediate products from these algorithms and their associated effects on the resulting image quality metrics can be used to provide information about environmental phenomena that may cause incoherence over the time scales observable in SAS data.

2 TEMPORAL VARIABILITY OF SAS DATA

SAS data can be used to observe changes in the acoustic response over multiple time scales. Data collected to aid motion estimation and compensation can be used to evaluate the coherence in the imaged area over consecutive sonar transmissions, while the quality of the imagery will be related to the level of coherence in the data comprising the synthetic aperture (after motion estimation and compensation and/or autofocus). Finally, an imaged area can be resurveyed and the coherence between the two images can be evaluated to measure the coherence over longer timescales[7]. Since other sonars can be used for measures of coherence across consecutive pings or in the resurvey of an area, the application of motion estimation techniques will only be briefly discussed and the remaining analysis included in this paper will focus on relating image quality metrics to coherence across the synthetic aperture.

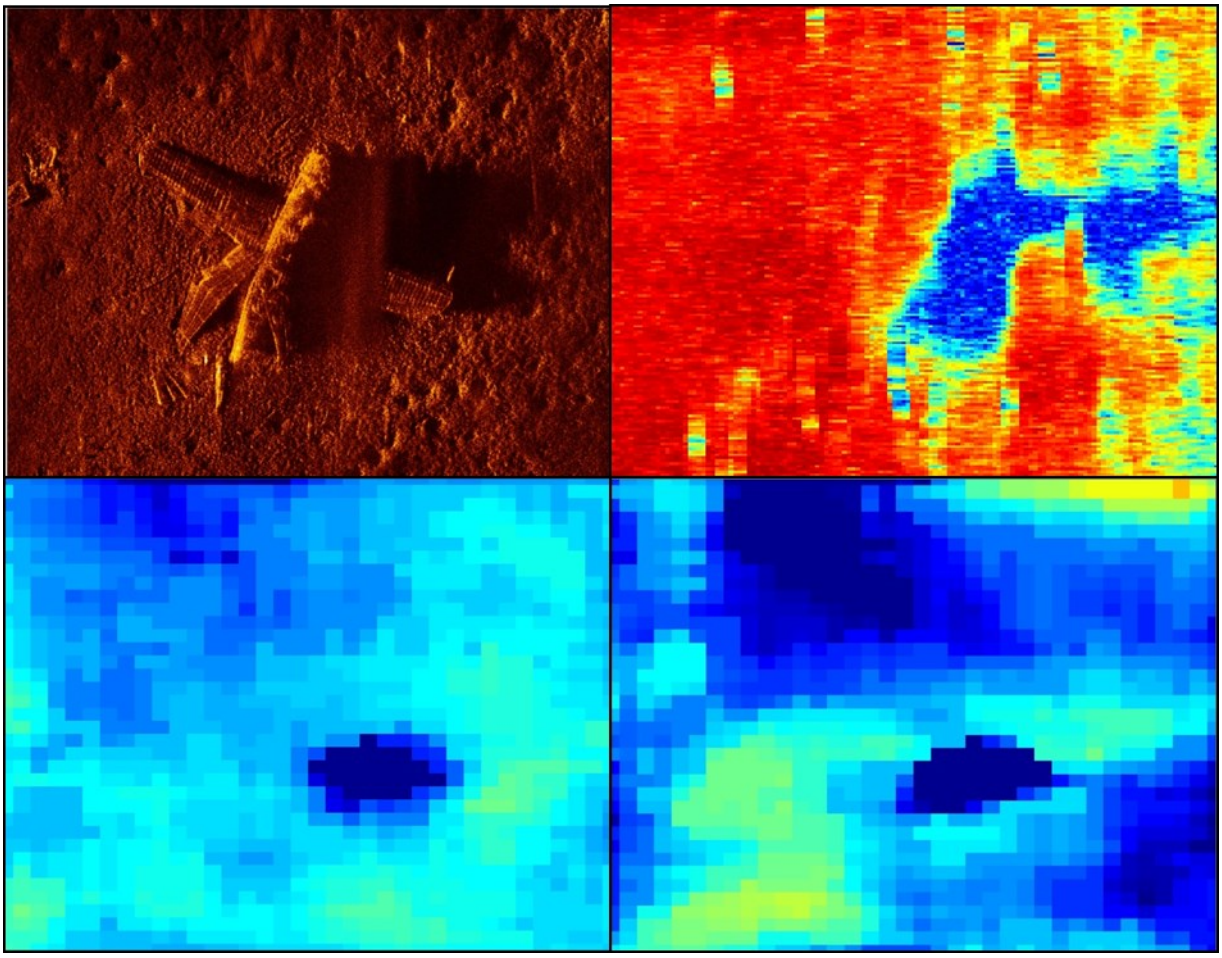

Figure 1: An example of a high-resolution SAS image (A, top left), the correlation coefficient from a comparison of RPC data from the image in A (B, top right), the range-axis image resolution for the image in A (C, bottom left), and the cross-range image resolution for the image in A (D, bottom right). The color in B corresponds to a correlation coefficient of 0 (blue) to 1 (red). The color in C and D correspond to the resolution expressed as a fraction of the theoretical limit scaled from 1 (blue, realized value at theoretical limit) to 2 (red, realized value twice the theoretical limit).

2.1 Coherence across consecutive pings

SAS systems often rely on a redundant phase center (RPC) motion estimation approach[6]. In this approach, the pulse repetition frequency is set such that the forward elements the array for one sonar transmission overlap in space with the aft elements of the next consecutive transmission. The resulting data includes array element data from adjacent pings collected from approximately the same point in space. The unwanted motion of the array between adjacent sonar transmissions can be determined by measuring the relative delay between the two redundant response signals. This delay is often determined using a cross correlation of the two signals and estimating the shift.

While primarily designed to evaluate system motion, RPC data can also be used for measuring the coherence of acoustic responses across consecutive transmissions. While the delay is used for motion analysis, the correlation coefficient can be used to identify areas of low coherence. An example of this can be seen in Figure 1B which shows the correlation coefficient from analysis of the RPC data associated with the SAS data used to form the image in Figure 1A. Reduced coherence can be observed in the shadow directly behind the airplane, in the areas of multi-path occurring within the fuselage (the smeared return directly behind the airplane), and a general trend of lower coherence with increasing range towards the far right of the image (onset of multipath associated with a surface bounce).

2.2 Coherence across the synthetic aperture

The point spread function of a point object or resolution (described here as the width of the point spread function 3dB from the peak intensity) within the field of view of a sonar is affected by the characteristics of the sonar and algorithms used during beamforming. The range-axis response is affected by the compression of the transmitted pulse and can be predicted from the transmitted bandwidth[2,8]. The range-axis resolution is largely unaffected by instabilities in the environment or motion since pulse compression occurs over very short time scales (the duration of the transmitted pulse). Unlike range-axis resolution, cross-range resolution can be dramatically affected by environmental factors or motion. The cross-range response of a point object is determined during beamforming and can be predicted from the aperture length[2,8]. However, incoherent samples in the synthetic aperture violate the assumptions in beamforming algorithms and will result in corruption of the ideal point spread function (*e.g.* wider central peak and increased side lobes). This can be seen in SAS imagery where uncorrected motion errors cause blurring and a loss of image contrast.

The resolution of a point response in both the range and cross-range dimensions can be measured by selecting a subset of the data around the point object and simply measuring the width of the peak. Unfortunately, an idealized point object rarely exists in nature and calibrated targets cannot capture subtle differences in resolution across an image. One method to estimate the resolution variability in an image that has been demonstrated is to take a statistical approach by assuming all bright objects are idealized point objects, measuring the peak widths, and locally average or otherwise smoothing the results to reduce the associated errors[5]. Previous research using this approach to evaluate image resolution demonstrated the relationship between aperture length, bandwidth, and the response of the image metrics and further related a decrease in cross-range resolution with incoherence along the synthetic aperture[5] presumed to be caused by unresolved sensor motion.

Incoherent samples along the synthetic aperture present during beamforming will result in changes in image contrast beyond its effect on the resolution of bright objects. At the other end of the intensity scale, one could examine the shadow depth in order to gain information regarding synthetic array coherence and the resulting image quality[9,10]. In a case where the phase of samples along a synthetic aperture are not accurately modeled under the assumptions of the beamforming algorithms, the point response of nearby scattering objects will blur into shaded regions, reduce the prevalence of low-intensity pixels in the image, and decrease mean shadow depth

3 COHERENCE ESTIMATES FROM MODELED SAS DATA

A data set with precisely known areas of incoherence was not available for analysis. Therefore, a sample with no known abnormalities was used as a basis for experimentation. This dataset was then modified to produce a quadratic phase error along the synthetic aperture and a new image was created with the specified error. This process was repeated with a range of errors that correspond with up to a +/- 0.5*λ shift relative to the geometry assumed in beamforming where λ is the wavelength of at the center frequency of the transmitted band. Since a quadratic phase error was applied, the error would be zero at the point of closest approach and increase along a quadratic trajectory achieving the stated maximum value at the outside edges of the synthetic aperture. Finally, image statistics were calculated for the set of images that describe the resulting resolution and shadow contrast. All image statistics were measured relative to the control image: range and cross range resolution are determined using the statistical method described in section 2.2 and expressed relative to the control. Shadows were identified as pixels with the lowest 0.1% of intensities of the control image. Shadow depth was measured as the mean intensity of shadow pixels relative to the mean of the same pixels in the control image.

The control image selected for analysis is shown in Figure 1A. A qualitative analysis of Figure 1A shows a well-focused image with a dynamic range typical for this system under good motion and environmental conditions. This qualitative analysis that the control image is relatively free of errors

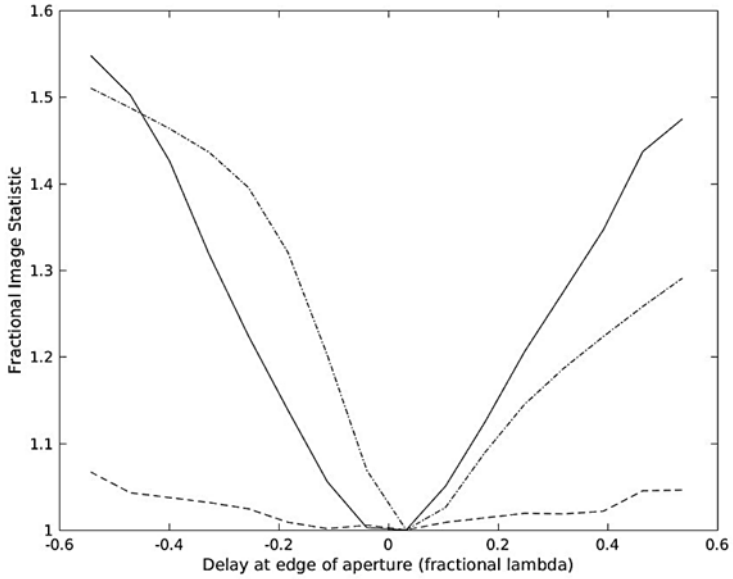

Figure 2: The response of relative image statistics to quadratic phase error along the synthetic aperture for a SAS system. The error shown is the shift in the geometry assumed by the beamforming algorithms at the outside edges of the synthetic aperture expressed as a fraction of λ. The solid line represents realized cross-range resolution relative to optimal, the dashed line represents realized range resolution relative to optimal, and the dot-dashed line represents shadow contrast relative to optimal.

associated with local incoherence is consistent with the resolution results. The results from a resolution analysis of the image are shown in figures 1C (range resolution) and 1D (cross-range resolution). These results indicate that both the range and cross-range resolutions are relatively consistent over the image and near the theoretical limits for the system used to acquire the data.

The results from analysis of the imagery with known incoherence are shown in Figure 2, which illustrates the degradation in image quality with increasing levels of incoherence. The resolution can be seen to degrade by a factor of ~1.5 in the cross range dimension when a quadratic phase error is introduced with a maximum deviation of 0.5λ. Under the same conditions, the range resolution is relatively unchanged. This is to be expected since the range resolution is primarily related to the transmitted bandwidth, which was not altered by the injected phase error. This result also provides some confidence that the resolution measurement is not biased by the phase modification. The cross-range resolution results are similar to what one would expect in a case where the synthetic aperture is shortened. However, the shadow depth metric responds similarly to the resolution metric indicating that incoherent noise is corrupting the beamforming results. If the aperture length was shortened (or a window was applied to the spectral bandwidth) in order to reduce resolution, the shadow depth would not degrade as in the example above.

4 COHERENCE ESTIMAGES FROM IN SITU SAS DATA

Image quality metrics were applied to imagery with obvious indications of environmental instabilities. The selected test image is shown in Figure 3 which depicts a relatively flat seafloor with a single box shaped object. A qualitative analysis of the section around the box shaped object indicates that the image is relatively well focused, but not as finely focused as the control image. A careful review of the motion statistics indicates that there is some unresolved motion, primarily an oscillating surge term that is causing the observed motion induced blur. However, the most prominent feature of the imagery is the large wave-like ripples that occur in the far range of the image. Since this area is known to be relatively flat from other survey data including different aspects times, it can be concluded that this image feature is related to environmental phenomena. Others have observed similar structures and have attributed their presence to internal breaking

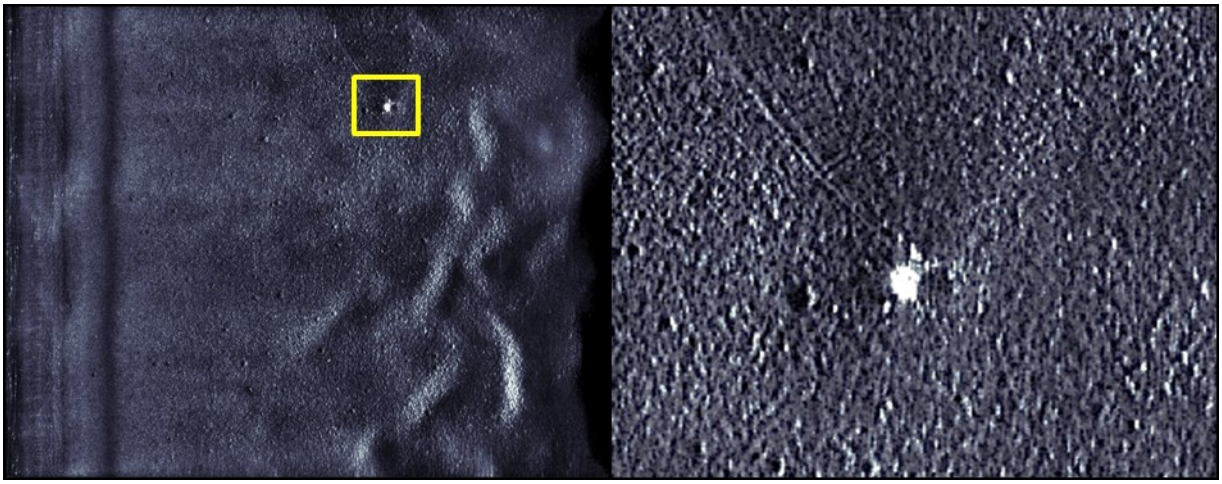

Figure 3: An image including environmental instabilities (left) and an enlarged section of the yellow box in the left image (right). While the right image indicates that the image is well focused, the ripple structure in the left image is due to environmental phenomena (i.e. the seafloor is actually flat).

waves and refraction caused by the boundary between the two water bodies with differing sound velocities[11,12].

An interferogram was made from the test image data to determine if the observed phenomena was altering the phase of SAS data. The SAS system used for data collection is equipped with two vertically separated imaging arrays and the difference in the phase between the two vertically separated images is shown in Figure 4C. While phase is shown in this image, the results could be easily translated to seafloor height if the assumptions in the calculations were not violated by the environmental conditions. In this image, blue areas would correspond to seafloor below the mean and red above the mean. While on first glance this might appear to be consistent with an actual rippled surface, there are areas where this relationship is reversed (blue areas on what would appear to be a ripple peak). This becomes more apparent with the peak and trough areas overlaid on the image Figure 1D.

Resolution measurements were conducted on the test image to determine if the ripple structure observed in the imagery corresponded to decreased coherence along the synthetic aperture. The results of this analysis are shown in Figure 4B which shows an overlaid map of the cross-range resolution on an enlarged section of the ripple structure. Areas where the local resolution is greater than twice the image mean are shown in red. These areas correlate well with the bright areas of the image. There are areas present with poor resolution that do not correlate with the rippled structure, primarily the horizontal area approximately in the center of the figure. This feature correlates with poor resolution in the imagery due to uncorrected system surge similar to that previously identified in Figure 3.

The response of shadow depth to the apparent areas of incoherence was not evaluated for this image. The environmental phenomenon observed includes areas of highlight and shadow that do not correspond to the actual seafloor geometry. This is likely due to refocusing the energy creating the illusion of an irregular seafloor. Therefore, the energy present in this area of the image is highly influenced by the lensing effect described above, which would confuse any attempt to relate shadow depth with environmentally induced incoherence.

5 CONCLUSIONS

The primary objective of this research was to determine if image quality metrics can be used to provide information about environmental phenomena that may cause incoherence over the time scales observable in SAS data. While the results illustrate utility when comparing the image

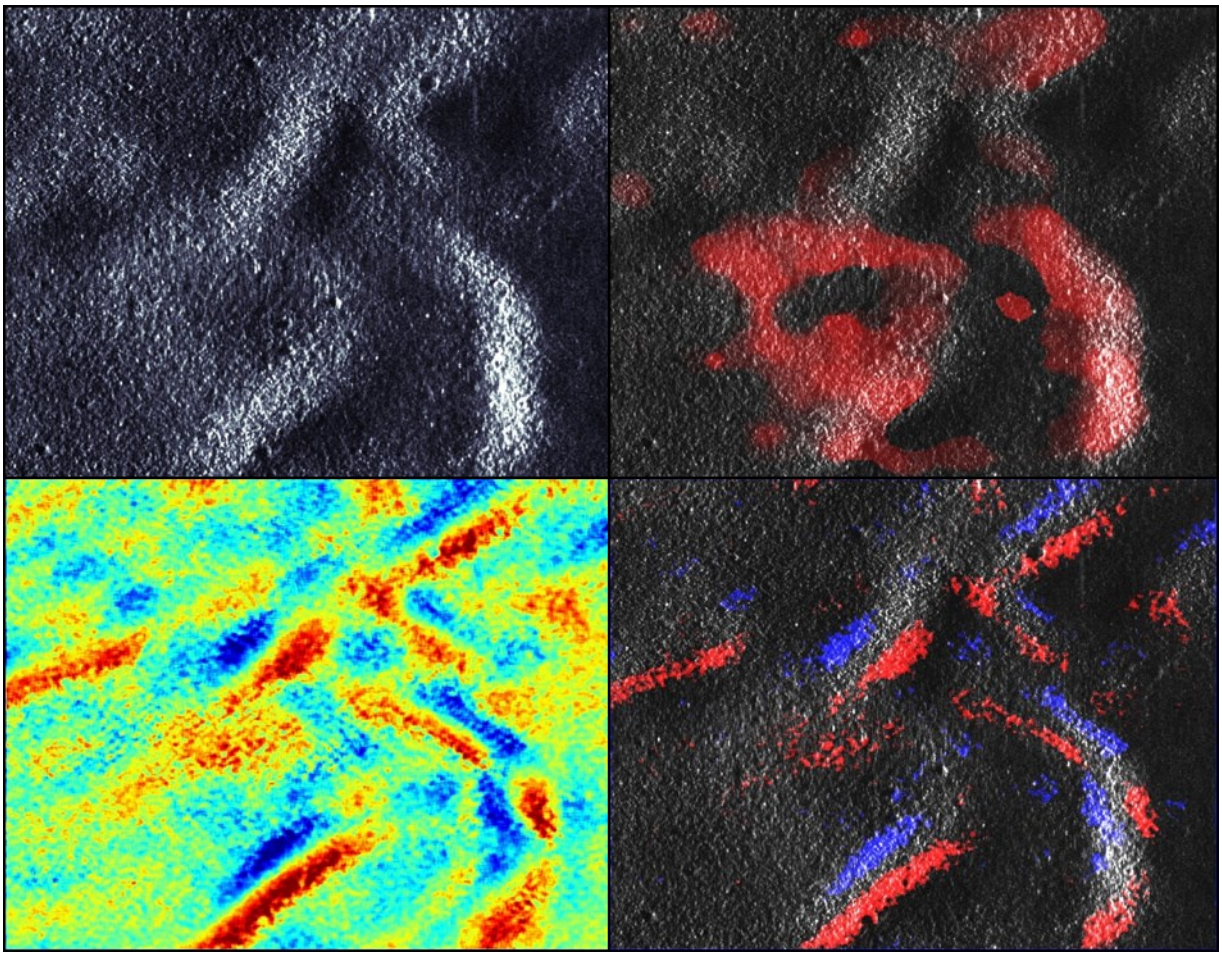

Figure 4: An enlarged image of the rippled area from the image in Figure 3 (A, top left), the same image with the areas of poor resolution overlaid in red (B, top right), an interferogram of the imaged area (C, bottom left), and the peak and troughs of the interferogram overlaid on the image (D, bottom right).

resolution with likely areas of incoherence, the measurement is confused by the inclusion of uncorrected platform motion associated errors. Care must be taken to separate environmental factors from other known sources of blurring. Furthermore, automatically driven algorithms that correct phase irregularities to focus imagery could obscure any environmentally driven blurring. However, careful implementation of these techniques could be used to both produce well focused imagery and identify environmental sources of incoherence. For example, autofocus phase corrections could be stored and translated back to array positon. Multiple position measurements would be available for array element positions and disagreement between position estimates could be attributed to environmental phenomena.

As we discuss incoherence, it is important to point out that incoherence exists where the assumed physical model of the data does not match reality. In this, identification of areas of incoherence is important because it can shed light on what we do not understand. The phase abnormalities caused by the environmental phenomena in the test data are clearly not noise. The pattern evident in the interferogram indicates that there is further information present in the phase (or deviation of the phase from assumed relationships in beamforming). Future research could exploit these deviations to gain additional insight on observed phenomena and use this information to both improve image formation and provide high resolution environmental measurements.

6 ACKNOWLEDGMENT

The authors would like to express gratitude to Dr. Jason Stack at the Office of Naval Research and Mr. Jose E. Fernandez at the Naval Surface Warfare Center Panama City Division for providing guidance with development of this project.

7 REFERENCES

1. R. J. Urick, Principals of Underwater Sound, 3rd Edition, McGraw-Hill Book Company, New York, 1983.
2. D. W. Hawkins: Synthetic Aperture Imaging Al-gorithms: with application to wide bandwidth sonar, PhD thesis, Department of Electrical En-gineering, University of Canterbury, Christ-church, New Zealand, 1996.
3. D.D. Sternlicht, J.E. Fernandez, T.M. Marston, “Detecting, Classifying Mines With Synthetic Aperture Acoustic Tomography”, Sea Technology, vol. 53, Issue 11, pp.10, November 2012,
4. O. Midtgaard, I. Alm, T.O. Saebo, M. Geihufe, R.E. Hansen, “Performance Assessment Tool for AUV Based Mine Hunting’, Proceedings of the Institute of Acoustics, vol. 36, Pt. 1, 2014.
5. J. L. Prater, J. L. King, D. C. Brown, ”Determination of Image Resolution from SAS Image Statistics”, MTS/IEEE Oceans ’15 Washington D.C., October 2015.
1. D.A. Cook, “Synthetic Aperture Sonar Motion Estimation and Compensation”, Thesis, Georgia Institute of Technology, May 2007.
7. T. G-Michael, B. Marchand, J.D. Tucker, T.M. Marston, D.D. Sternlicht, M.R. Azimi-Sadjadi, “Image-Based Automated Change Detection for Synthetic Aperture Sonar by Multistage Coregistration and Canonical Correlation Analysis”, IEEE Journal of Oceanic Engineering, 41, pp.592-612, July 2016.
8. M. Soumekh: Synthetic Aperture Radar Signal Processing with MATLAB Algorithms John Wiley and Sons, Inc., 1999.
9. D.A. Cook, D.C. Brown, “Analysis of Shadow Contrast for Synthetic Aperture Sonar Imagery”, Proceedings of the Institute of Acoustics, vol. 32, no. 4, 2010.
10. D. Cook, D. Brown, Z. Lowe, “Synthetic Aperture Sonar Contrast”, 1st International Conference and Exhibition on Underwater Acoustics, Greece.
11. R.E. Hansen, A.P. Lyons, D.A. Cook, T.O. Saebo, “Detection of Internal Waves Using Multi-Aspect Processing in Synthetic Aperture Sonar”, 11th European Conference on Synthetic Aperture Radar EUSAR, Hamburg, Germany.
12. R.E. Hansen; A.P. Lyons, T.O. Sæbø, H. Callow, J. Hayden John, and D.A. Cook,”The Effect of Internal Wave-Related Features on Synthetic Aperture Sonar”, IEEE Journal of Oceanic Engineering. ISSN 0364-9059. 40(3), s 621- 631 . doi: 10.1109/JOE.2014.2340351 2015.